Available online at www.sciencedirect.com
ScienceDirect
Energy and Buildings 39 (2007) 221–235
ENERGY and BUILDINGS
www.elsevier.com/locate/enbuild

Impact of adaptive comfort criteria and heat waves on optimal building thermal mass control

Gregor P. Henze [a,*], Jens Pfafferott [a], Sebastian Herkel [a], Clemens Felsmann [b]

[a] *Fraunhofer Institute for Solar Energy Systems, D-79110 Freiburg, Germany*
[b] *Technical University of Dresden, Institute for Thermodynamics and Building Systems Engineering, D-01069 Dresden, Germany*

Received 4 May 2006; received in revised form 15 June 2006; accepted 20 June 2006

Abstract

This article investigates building thermal mass control of commercial buildings to reduce utility costs with a particular emphasis on the individual impacts of both adaptive comfort criteria and of heat waves. Recent changes in international standards on thermal comfort for indoor environments allow for adaptation to the weather development as manifested in comfort criteria prEN 15251.2005 and NPR-CR 1752.2005 relative to the non-adaptive comfort criterion ISO 7730.2003. Furthermore, since extreme weather patterns tend to occur more frequently, even in moderate climate zones, it is of interest how a building's passive thermal storage inventory responds to prolonged heat waves. The individual and compounded effects of adaptive comfort criteria and heat waves on the conventional and optimal operation of a prototypical office building are investigated for the particularly hot month of August 2003 in Freiburg, Germany. It is found that operating commercial buildings using adaptive comfort criteria strongly reduces total cooling loads and associated building systems energy consumption under conventional and building thermal mass control. In the case of conventional control, total operating cost reductions follow the cooling loads reductions closely. Conversely, the use of adaptive comfort criteria under optimal building thermal mass control leads to both lower and slightly higher absolute operating costs compared to the optimal costs for the non-adaptive ISO 7730. While heat waves strongly affect the peak cooling loads under both conventional and optimal building thermal mass control, total cooling loads, building energy consumption and costs are only weakly affected for both control modes. Passive cooling under cost-optimal control, while achieving significant total cost reductions of up to 13%, is associated with total energy penalties on the order of 1–3% relative to conventional nighttime setup control. Thus, building thermal mass control defends its cost saving potential under optimal control in the presence of adaptive comfort criteria and heat waves.

Keywords: Low-energy office buildings; Thermal comfort; Adaptive comfort models; Cooling energy; Thermal mass control; Night ventilation; Weather data analysis; Heat waves

1. Introduction

Cooling of commercial buildings during hot summer periods places a considerable peak demand on an electrical utility grid; electrical demand and time-of-use (TOU) utility rates are designed to encourage shifting of electrical loads to off-peak hours. Typically on-peak hours are enforced during business working days, and off-peak hours at night and on weekends. The standard building control strategy, termed nighttime setup temperature control, operates the building temperature within a comfort range during occupancy; when the building is unoccupied the temperature setpoint is set to a high value and the space temperature is allowed to float. This control strategy ignores the thermal capacitance of the building structural mass that could be harnessed to reduce cooling-related operating costs because the building structural mass represents a passive building thermal storage inventory that can serve as a heat sink.

As an illustration, passive cooling has a long history in European architecture where the more moderate climate allows for the building itself to be harnessed as a thermal storage system with the opportunity to reduce the need for chilled water equipment. Current European building designs employ large areas of exposed building mass, solar control using actuated external shading devices, nighttime ventilation, and ground-coupled heat pumps.

The basic principle of building precooling is to run the chiller and air-handling equipment during off-peak hours to charge the thermal mass and to use air-side free cooling to the extent available. During occupancy the optimal controller

* Corresponding author.
E-mail address: ghenze@mail.unomaha.edu (G.P. Henze).

0378-7788/$ – see front matter © 2006 Elsevier B.V. All rights reserved.
doi:10.1016/j.enbuild.2006.06.006

maintains temperature and/or humidity within specified ranges. Throughout the expensive on-peak period, the thermal mass is discharged to reduce mechanical cooling and thus electrical consumption and demand requirements. By setting building zone temperature setpoints in an appropriate (possibly optimal) fashion, the passive storage inventory is harnessed and the resultant thermal load shifting will help reduce costly on-peak electricity consumption and demand and thus reduce operating costs. Furthermore, building thermal storage inventory for both heating and cooling will gain importance as it offers the possibility to more strongly utilize uncontrolled renewable energy sources such as wind and solar.

The purpose of this article is to evaluate the potential of optimal control for passive thermal energy storage to reduce utility costs with a particular emphasis on the impacts of comfort criteria and heat waves. Recent changes in pertinent international standards on thermal comfort for indoor environments allow for some adaptation to the weather development, i.e., they account for the human's ability to adapt to persistently hot or persistently cold weather periods. Changes in allowable temperature limits for the indoor environment will thus affect the energy consumed to operate the building energy systems under both conventional (nighttime setup) and optimal precooling operating strategies. Moreover, extreme weather patterns tend to occur more frequently even in moderate climate zones [23]. This article will assess the individual and compounded effects of adaptive comfort criteria and heat waves on the conventional and optimal operation of a prototypical office building for the particularly hot month of August 2003 in Freiburg, a city located in southwest Germany.

2. Methodology

To investigate the impact of adaptive comfort criteria and weather pattern stability (summer heat waves) on building thermal mass control, we adopted the following methodology:

(1) Selection of a representative low-energy office *building model* with respect to the building structure, HVAC systems, and building utilization (low internal gains and external shading devices).
(2) Selection of *weather data* that contain sufficiently extreme features both in terms of average temperature as well as the occurrence of multi-day heat waves. Two distinct data sets, one with and one without heat waves, are generated from this weather data file.
(3) Calibration of the building model with *measured data from an actual building*, the Fraunhofer Institute for Solar Energy Systems located in Freiburg, Germany, to investigate whether the building adopted for this study is suitable for the application of adaptive comfort criteria. The purpose of this comparison is confirm whether the building model adopted behaves similarly to an actual passively cooled building. Moreover, we adopted the rationale that a building that would be considered suitable for passive cooling would also be considered suitable for adaptive comfort criteria when actively conditioned.
(4) Selection of three *comfort criteria*: ISO 7730.2003 as the internationally accepted (non-adaptive) standard on thermal comfort; prEN 15251.2005 and NPR-CR 1752.2005 as two adaptive thermal comfort criteria.
(5) Conducting *monthly simulation runs* for both conventional nighttime setup control as the reference case and optimal building thermal mass control for the selected two weather data sets and three comfort criteria.
(6) The *evaluation of the results* is conducted by means of a monthly energy cost analysis utilizing a dynamic building energy simulation program coupled to a popular technical computing environment. Quantitative comparisons will be presented for the conventional strategy (nighttime setup control) as the reference strategy and the cost-optimal building thermal mass precooling strategy.
(7) Deriving *general conclusions* from the individual results.

3. Review of building thermal mass control

3.1. Modeling results

Several simulation studies have shown that proper precooling and discharge of building thermal storage inventory can attain considerable reductions of operating costs in buildings. These savings result from both utility rate incentives (time-of-use and demand charges) and improvements in operating efficiency due to nighttime free cooling and improved chiller performance (lower ambient temperatures and more even loading). Ranges of 10–50% in energy cost savings and 10–35% in peak power reductions over night setup control were documented in a comprehensive simulation study [1]. The savings were highest when cool ambient temperatures allowed for free cooling. Other modeling studies yielded similar results [2–6]. Common to these simulation studies is that the level of savings and the superior control strategy strongly depend on the investigated HVAC system and on the climate. For the references cited in this section, peak energy cost savings for cooling were 10–30%, whereas maximum HVAC electrical demand was reduced by as much as 40% depending on the optimization cost function. Yet, improper application of precooling could actually result in costs that exceed those associated with conventional control.

3.2. Experimental results

A few controlled laboratory experiments have been conducted to demonstrate load shifting and peak reduction potential associated with the use of building thermal mass. An experimental facility at the National Institute of Standards and Technology (NIST) was used to study the use of building thermal mass to shift cooling loads [7]. Several heuristic strategies were evaluated in the facility that was designed to represent a zone in a small commercial office building and configured as an interior zone without ambient coupling. Compared to night setup control, peak cooling demand was lowered by up to 15%.

A more recent set of experiments performed at NIST validated the potential for load shifting and peak cooling load reduction associated with optimal control [8]. Here, a model of

the test facility was developed and validated that included detailed models of the building structure, cooling system, and human comfort. Optimization techniques were applied to the simulation model to determine control strategies used in the two separate tests. The first control strategy was designed to minimize total energy costs and resulted in the shifting of 51% of the total cooling load to the off-peak hours. The second control strategy was designed to minimize the peak electrical demand and resulted in a 40% reduction in peak cooling load. Thermal comfort was maintained throughout both experiments.

A small number of field studies have been conducted as well. Two experiments on building precooling were conducted in an office building in Florida without optimizing the storage [9] where 18% of the total daytime cooling load was shifted to the night period. Keeney and Braun [10] investigated a control strategy that utilizes building thermal mass to reduce peak cooling requirements in the event of the loss of a chiller. The control strategy was tested in a 1.4 million ft^2 (130,000 m^2) office building located near Chicago, IL. The facility consists of two identical buildings with near-identical internal gains and solar radiation loads that are connected by a large separately cooled entrance area. During tests, the east building used the existing building control strategy while the west building used the precooling strategy. As expected from simulation predictions, the precooling control strategy successfully limited the peak load to 75% of the cooling capacity for the west building, while the east building operated at 100% of capacity.

Braun et al. [11] reported findings of simple precooling tests performed at the Iowa Energy Center. This facility is used for performing research on building controls and diagnostics and is very well instrumented and maintained. A sequence of 2-week long tests was performed using a conventional night setup and a simple precooling control strategy. The cumulative occupied load for the test zones was 23% less for the precooling strategy than for night setup control.

Pfafferott et al. [12] evaluated the efficacy of a passive cooling concept employing nighttime ventilation for the Fraunhofer ISE building, which will be further adopted as the reference building for model calibration in this study. For further information on model-based evaluation of monitored passively cooled commercial buildings, refer to Ref. [13].

3.3. Optimal control of passive thermal storage inventory

A simplified method was developed based on simulation that defines the optimal zone temperature setpoints to minimize daily energy costs over a 24-h period and subsequently reduced this problem to the determination of only two variables [6]. Calculation of the energy costs did not include utility demand charges. The simplified method compared favorably with the more detailed benchmark approach by [8] that involves the optimization of 24 variables for each zone (the zone temperatures for each hour of the day). Energy cost savings between 22 and 42% were achieved dependent on the average ambient temperature; higher fractional savings can be achieved with precooling on cooler days. Moreover, Henze et al. [14] conducted experiments of real-time predictive optimal control of active and passive building thermal storage inventory in the Energy Resource Station and found significant reduction of on-peak demand on the order of 70% in response to building precooling in spite of the fact that the building does not embody large amounts of thermal capacitance.

Finally, Henze et al. systematically evaluated the merits of the passive building thermal capacitance to minimize energy cost for a design day using optimal control [15]. The optimal controller predicts the required extent of precooling (zone temperature setpoint depression) depending on utility rate structure, occupancy and on-peak period duration and onset, internal gains, building mass, occupancy period temperature setpoint range, and weather as characterized by diurnal temperature and relative humidity swings.

From the aforementioned simulated and experimental results, it has been shown that thermal loads can indeed be shifted and cost savings attained. The effective utilization of thermal mass requires that the control strategy be suited to the problem, and therefore optimized. Inappropriate control strategies could result in increased cost and energy use, as observed in the discrepancy of results between Conniff and Morris. The optimal control in this study is based on perfect weather forecasts and model knowledge, and thus the actual cost savings will be less than the theoretical projected savings. For the impact of forecasting uncertainty and modeling mismatch on optimal control, Refs. [16–18] should be consulted.

Finally, Braun surveyed research on passive building thermal storage utilization in commercial buildings [19]. He identified considerable saving potential for operating costs, even though the total zone loads may increase. Opportunities for reducing operating expenses are due to four effects: reduction in demand costs, use of low cost off-peak electrical energy, reduced mechanical cooling resulting from the use of cool nighttime air for ventilation precooling, and improved mechanical cooling efficiency due to increased operation at more favorable part-load and ambient conditions. However, these benefits must be balanced with the increase in the total cooling requirement that occurs with the precooling of the thermal mass. Therefore, the savings associated with load shifting and demand reduction are very sensitive to utility rates, building and plant characteristics, weather conditions, occupancy schedules, operating condition, the method of control, and the specific application. In general, better opportunities for effective precooling exist for higher ratios of on-peak to off-peak rates, longer on-peak periods, heavy-mass building construction with a small ratio of the external area to the thermal mass, and for cooling plants that have good part-load characteristics for which the best performance occurs at about 30% of the design load.

4. Description of the building model

Two essential assumptions are applied: (a) weather, occupancy, and non-cooling electrical loads are perfectly predicted; and (b) the building thermal response is perfectly represented by the building model, i.e., there is no mismatch between the modeled and actual building behavior.

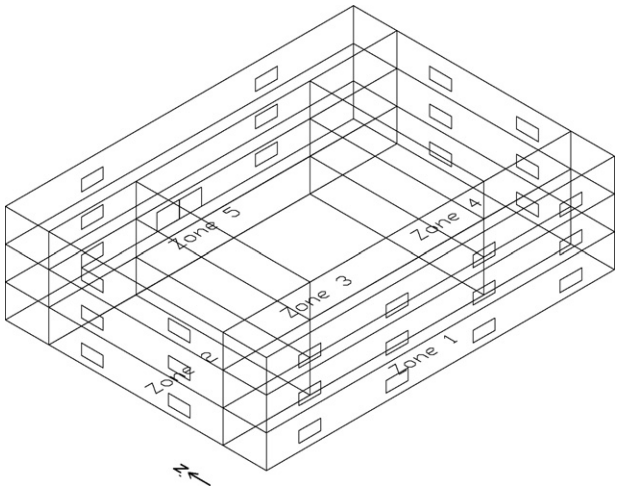

Fig. 1. Isometric view of office building.

4.1. General building features

The model of a three-story office building located in Freiburg, Germany is investigated in this study. The isometric view as shown in Fig. 1 reveals five thermal zones per floor, i.e., 15 thermal zones in total. The perimeter zones have an area of 288 m^2 each, while the core zone has an area of 576 m^2. Total area per floor is thus 1728 m^2 and the building total is 5184 m^2.

In an effort to calibrate the simulation building model with an actual naturally ventilated building characterized by a high building thermal mass, the Fraunhofer Institute for Solar Energy Systems (ISE) located in Freiburg, Germany was selected as the reference building. Table 1 compares the most important building features of the simulation model and the Fraunhofer ISE building in Freiburg, Germany.

With respect to the building simulation model, counting the exterior envelope, floor, and ceiling surfaces, the building mass is approximately 770 kg/m^2 of floor area, and thus can be considered heavy-weight construction. Table 2 shows the thermal characteristics of the exterior walls, interior partitions, ceilings, and floors for this study.

Table 1
Comparison of central building features

Feature	Units	Model	Fraunhofer ISE
Surface-to-volume ratio	[1/m]	0.25	0.31
Window fraction	[−]	0.11	0.21
Gross floor area	[m^2]	5184	14000
Gross room volume	[m^3]	23328	64322
Mean *U*-value	[W/m^2K]	0.61	0.43

Table 2
Thermal characteristics of building model construction elements

Construction name	*U*-value [W/m^2K]	Capacitance [kJ/m^2K]
Exterior wall	0.64	252
Roof	0.47	425
Floor	0.51	1257
Ceiling	2.43	435
Interior wall	2.30	216

Peak building occupancy is 10 m^2/person. Each office occupant contributes 132 W of internal gain, of which 54% are assumed to be sensible and 46% latent. Peak lighting and equipment power density is 12 W/m^2 in the perimeter zones and 20 W/m^2 in the (windowless) core zones. Occupancy is assumed to last from 8:00 to 18:00, with the on-peak period beginning at 11:00 and ending at 21:00.

The building is equipped with an air-cooled reciprocating chiller (available in nominal capacities of 205–1445 kW) with a selected nominal capacity of $CCAP_{nom}$ = 500 kW. According to the manufacturer's data, the chiller has a nominal coefficient-of-performance (COP) of 3.07 [20], which exceeds ASHRAE Standard 90.1–2004 minimum requirement of 2.80. The zones are conditioned using a variable air volume (VAV) air-handling unit with electric reheat at the VAV terminal boxes. Zone temperatures are controlled by a dual setpoint controller with dead band. For conventional nighttime setback control, called ''reference case'' in this study, the system is off during the unoccupied hours and the indoor temperature is allowed to float; the system is on during occupied hours (8:00–18:00) and keeps the indoor temperature at the upper limit of cooling setpoints as governed by the comfort criteria of choice.

The outdoor airflow rate is controlled by a return air temperature based economizer that adjusts the outdoor air fraction from 0 to 100% by comparing the temperature of return air and outdoor air. At the same time, the outdoor air fraction must meet the schedule of minimal outdoor air fraction of 15% during occupied periods. For the reference case operation of nighttime setup control, outdoor air intake flow rates always exceed the required value of $\dot{V}_{ot} = 10,260\,m^3/h$ during occupied times as demanded by ASHRAE Standard 62.1–2004.

However, using optimal thermal mass control, ventilation rates during occupied periods are typically lower and will not necessarily always maintain minimum ventilation rates.

Supply air temperature is set to a constant value of 13 °C during the cooling season, i.e., no temperature reset control is applied. Henze et al. [15] presented a variation of daily electricity consumption and operating cost as a function of supply air temperature (SAT) between 11 and 16 °C. It was observed that by increasing SAT, the chiller power consumption is reduced while the fan power consumption increases sharply. Lower SAT leads to lower total energy consumption. To avoid discomfort problems in response to supplying excessively cold air, a SAT setpoint of 13 °C is selected as a comprise between energy efficiency and comfort.

Moreover, the AHU design airflow is 140,000 m^3/h with an associated design electrical demand of 93 kW for the supply fan and 48 kW for the return fan. Design supply air pressure drop is approximately 1500 and 750 Pa for the return air duct, representing a low pressure drop design. A simple affinity law relationship was adopted that assumes fan power consumption to vary with the cube of the flow part load ratio relative to the design conditions.

4.2. Passive thermal storage system modeling

The building structure responds to changes in zone temperature setpoints $T_{z,sp}$. The zone temperature T_z is directly affected only by the net convective heat flux according to the discrete-time energy balance on the zone air mass

$$C_z \frac{\Delta T_z}{\Delta t} = \sum_i \dot{Q}_{\mathrm{conv},i},$$

where C_z is the zone thermal capacitance. These convective heat fluxes include contributions from interior wall surfaces due to transmission and delayed release of solar gains, HVAC systems, internal gains, as well as infiltration. Of those, the current interior wall surface fluxes depend on a history of past inside and outside air and surface temperatures as well as inside and outside heat fluxes.

The zone temperature setpoints can be varied between 15 and 35 °C during unoccupied periods and between the upper and lower temperature bound during occupied periods as defined by the comfort criterion in effect. Building precooling reduces the convective contributions from inside surfaces during occupied periods by depressing the average envelope temperature during unoccupied periods. Multi-zone simulation was conducted using a highly validated building simulation engine employing the conduction transfer function method.

4.3. Chilled-water system modeling

In order to account for chiller efficiency variations due to changes in ambient weather conditions, the chiller model maps manufacturer's performance data for a packaged hermetic reciprocating liquid chiller with an air-cooled condenser. The nominal capacity is based on an ambient dry-bulb temperature of 35 °C and leaving chilled water temperature of 7 °C. Different operating temperatures are accounted for by using the manufacturer's tabulated data to formulate performance equations by linear regression. The coefficient-of-performance COP for various outdoor dry-bulb temperatures T_{db} conditions was determined to be:

$$\mathrm{COP}(T_{\mathrm{db},k}) = (1.61875 - 0.01751_{\mathrm{db},k})\mathrm{COP}_{\mathrm{nom}}$$

with a coefficient of determination of $R^2 = 0.995$ where the nominal COP in chilled-water mode was reported to be $\mathrm{COP}_{\mathrm{nom}} = 502.2/163.4 = 3.07$.

Operating the cooling equipment at part-load conditions is associated with an energy penalty that can be described by a quadratic function of the part-load ratio PLR

$$\mathrm{PLR}_k = \frac{\dot{Q}_{\mathrm{load},k}}{\mathrm{CCAP}_k},$$

where $Q_{\mathrm{load},k}$ is the cooling load and CCAP_k the chiller capacity in hour k. Furthermore, using manufacturer's data, the dependency of the chiller capacity CCAP_k at hour k on the outdoor air dry-bulb temperature $T_{\mathrm{db},k}$ can be modeled. A linear relationship was found from manufacturer's data for this study

$$\mathrm{CCAP}_k = \mathrm{CCAP}_{\mathrm{nom}}[1 + \delta\,(T_{\mathrm{ref}} - T_{\mathrm{db},k})],$$

where the nominal chiller capacity is $\mathrm{CCAP}_{\mathrm{nom}} = 500$ kW and the slope was found to be $\delta = 0.01/K$ (i.e., a 1%-loss of capacity for every Kelvin of ambient temperature increase) and the reference temperature is $T_{\mathrm{ref}} = 35$ °C.

The electrical chiller power input P_{el} at part-load is commonly expressed as a quadratic function of the part-load ratio

$$P_{\mathrm{el}} = \frac{\mathrm{CCAP}_k}{\mathrm{COP}(T_{\mathrm{db},k})}[x + y\mathrm{PLR} + z\mathrm{PLR}^2],$$

where the values of x, y, and z are determined from manufacturer's data. For example, the coefficients of a hermetic reciprocating liquid chiller according to the DOE-2 Manual [21] are $x = 0.088065$, $y = 1.137742$, and $z = -0.225806$. The fraction of full-load power consumed at any particular part-load for a particular ambient condition can be taken from Fig. 2.

4.4. Reference case and utility rate

Cost savings and energy consumption will be stated relative to the ''reference case'' (RC) that is characterized by a chilled water system that experiences the same internal gain and weather profiles and uses the same HVAC systems subject to the same utility rate structure as the corresponding optimized passive storage system. However, the passive building thermal storage inventory is not utilized: during occupancy, the cooling zone setpoints as defined by the comfort criterion in effect are maintained; during unoccupied times, the HVAC systems are turned off and the temperatures are allowed to float. The performance metric for all cases is the monthly time-of-use differentiated electrical utility cost for operating the office building.

For both reference and optimal control strategies, the on-peak period lasts from 11:00 to 21:00. The default off-peak rate is \$0.05/kWh (or Euro 0.05/kWh) and the default on-peak rate is \$0.20/kWh (or Euro 0.20/kWh), i.e., the utility rate ratio is

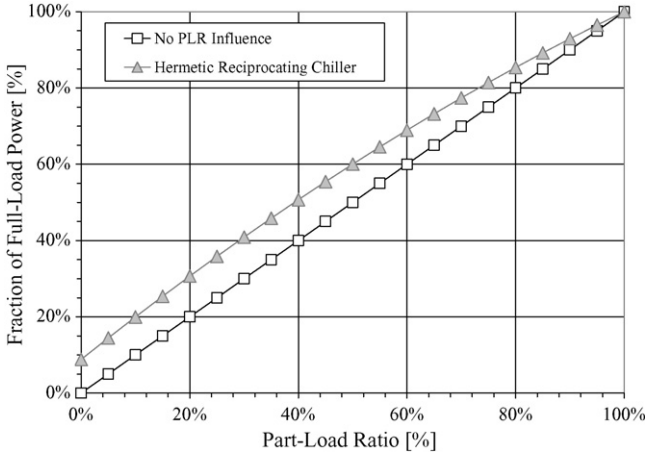

Fig. 2. Fraction of full-load power as a function of part-load ratio.

$R = 4$. The reference case is simulated with the same parameters as the respective optimal case; the only difference is that the reference case is always calculated for nighttime setup mode.

4.5. Weather conditions

The summer of 2003 was a historically hot summer in Europe with a particularly pronounced heat wave in early August. Most readers will recall news reports of 22,000 to 35,000 of heat-related deaths in France [22], particularly among the age groups above 45 years. Since the frequency of unusually hot summers with prolonged heat waves even in moderate climates is increasing according to Ref. [23], we are curious to learn to what extent these extreme weather conditions impact the potential savings from building thermal mass control.

While the summer of 2003 was hot as judged by the average dry-bulb temperature alone, it also featured several heat waves, the longest of which prevailed in early August of 2003. As the basis of our analysis, we therefore selected weather data for Freiburg, Germany for the period of July 30 through August 29, which is 31 days and thus 1 month of time. During this time period, the average ambient dry-bulb and wet-bulb temperatures were 25.18 and 17.53 °C, respectively. The average monthly ambient air temperature is already above typical cooling temperature setpoints for most commercial buildings, confirming the extreme conditions in 2003.

To better illustrate the climate in Freiburg, Germany and the drastic change in 2003, Fig. 3 presents contour plots of the relative frequency with which ambient temperatures and humidity ratios jointly occur. Darker shades correspond to more frequent events. From the left column of figures, it can be deduced that the standard climate as published by Meteonorm [24] for Freiburg, London, and Portland, Oregon are roughly similar. However, in 2003, the weather was so unusually hot for such an extended time period, that the Freiburg 2003 weather more closely resembles the climates of Rome or Salt Lake City.

We employed the weather data in two particular ways: first, we applied the original weather data including the heat wave as measured at the weather station. Second, we sliced the selected 31 days into individual days and concatenated the individual days in such a fashion that the heat wave was broken up into a series of hot days each followed by cooler days. Thus, we only changed the ordering of the days without changing monthly mean values for temperature, humidity, and insolation. A comparison of the original and manipulated temperature profiles (dry-bulb and wet-bulb) is shown in Fig. 4.

5. Standard and adaptive comfort criteria

The comfort criteria discussed in this article consider the comfortable room temperature RT_c [°C] as a function of the ambient air temperature AT [°C].

Comfort is evaluated based on the hourly mean room temperature and only for the time of occupancy, i.e., Monday to Friday, from 08:00 to 18:00. Each comfort criterion defines a temperature range around the comfort temperature RT_c which is a function of the occupant acceptance. (All criteria used in this study define comfort classes A, B and C.) The three comfort

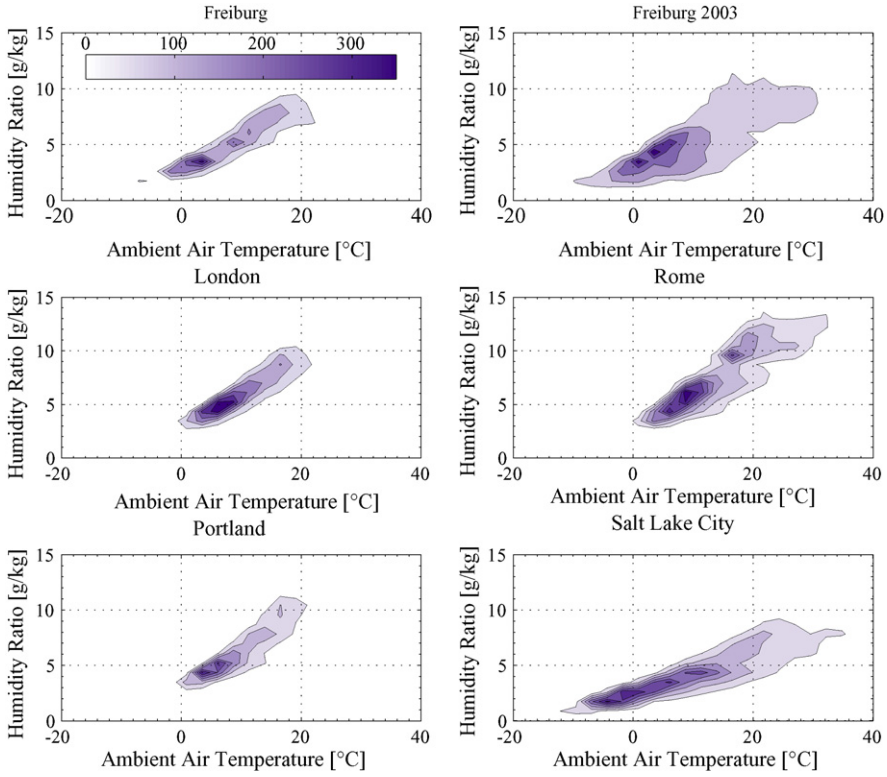

Fig. 3. Contour plots of temperature–humidity ratio histograms for Freiburg, London, Rome, Portland, and Salt Lake City based on Meteonorm [24] data and measured data for Freiburg in 2003. Darker shades correspond to more frequent events.

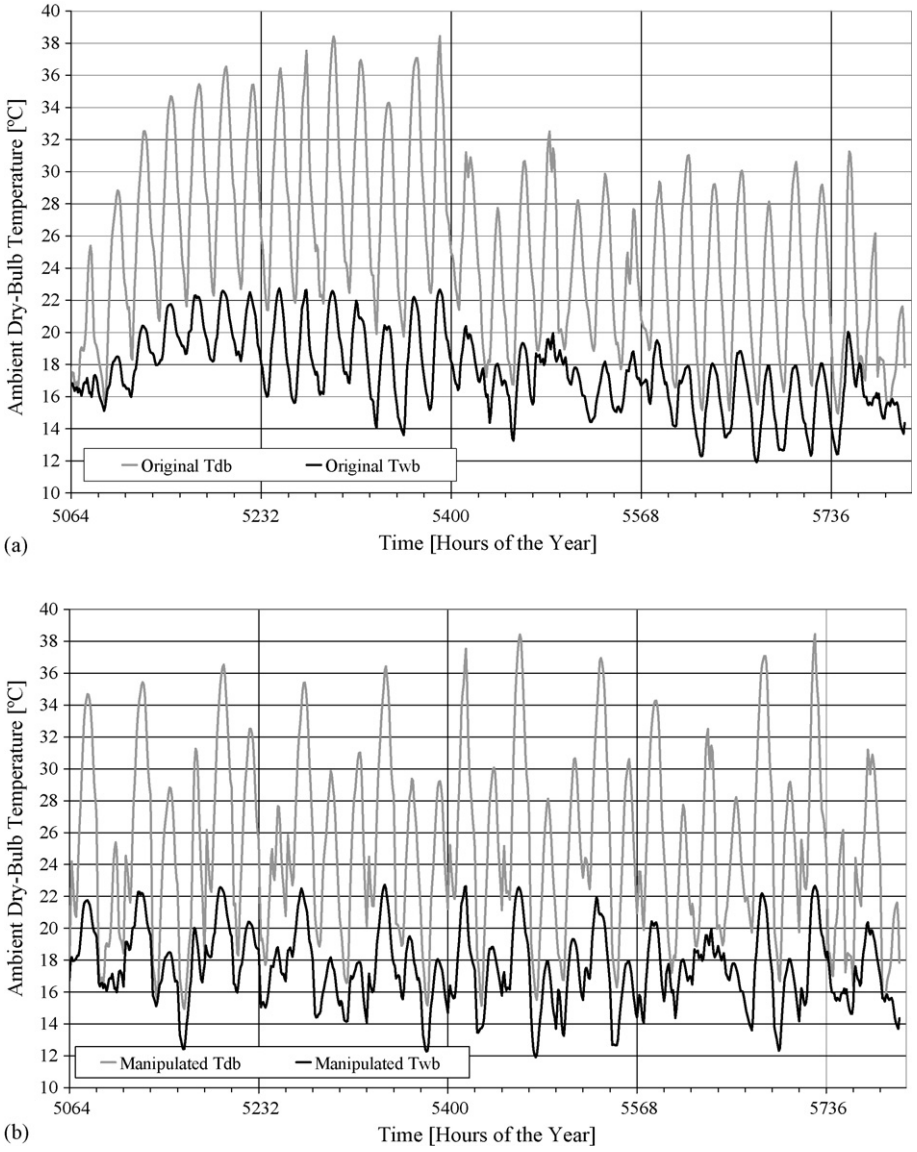

Fig. 4. (a) Original and (b) manipulated profiles for ambient air dry-bulb and wet-bulb temperatures for the Freiburg, Germany for the time period July 30 through August 29, 2003.

criteria consider different time periods of the ambient air temperature.

ISO 7730.2003 [25] distinguishes summer days from winter days. The comfort temperature RT_c is 22 °C in the winter and 24.5 °C in the summer. A ''summer day'' is defined by a minimum daily peak temperature of 25 °C according to the meteorological definition. All days in the summer of 2003 are thus summer days. The allowable comfort band for 90% occupant acceptance for ISO 7730 during summer periods is ±1.5 K around the comfort temperature.

prEN 15251.2005 [26] takes the monthly ambient air temperature AT_m into account. The comfort temperature is 22 °C in the winter and $RT_c = 17.8 + 0.31AT_m$ [°C] in the summer. The revised standard NPR-CR 1752.2995 [27] allows for thermal adaption of the building occupant as well. The comfortable room temperature responds to the moving average ambient air temperature of the past three days AT_{rm} using the same formula as prEN 15251 for high ambient temperatures but with another reference temperature: $RT_{c,hi} = 17.8 + 0.31AT_{rm}$ [°C]. The allowable comfort band for 90% occupant acceptance for prEn 15251 and NPR-CR 1752 during summer periods is ±2.5 K around the comfort temperature.

For the time period investigated in this study, during the very hot August of 2003 in Freiburg, Germany, the occupied period upper comfort limits for the three comfort criteria described above can be seen in Fig. 5.

6. Calibration of passive building response

Next, we investigated whether the building adopted for this study is suitable for the application of adaptive comfort criteria to be described below. To that end, we disabled the chiller and simply ventilated the building according to a fixed schedule of five ventilation air changes at night (23:00 to 7:00) and two

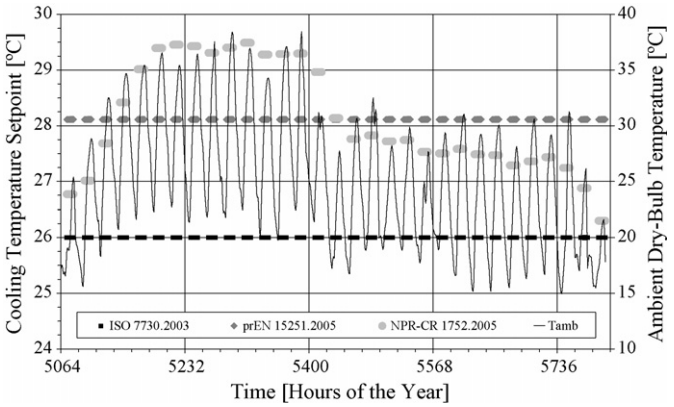

Fig. 5. Upper temperature limits for the three investigated comfort criteria during August 2003 in Freiburg, Germany.

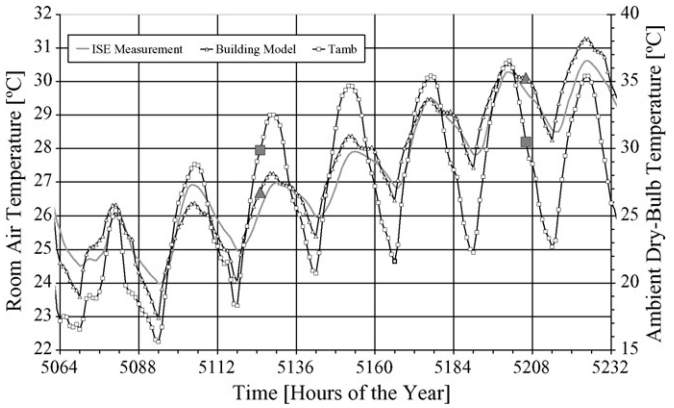

Fig. 7. Comparison of the passive building response for the building model and the Fraunhofer ISE using fixed ventilation schedules as a time history chart. Enlarged markers indicate room air temperature for the same ambient air temperature of 30 °C at the beginning and towards the peak of the heat wave.

ventilation air changes during the day (7:00 to 23:00). We compared the building response in terms of average room air temperature of the three southern zones in the model with the measured average room air temperature of 15 offices with southern exposure in the naturally ventilated Fraunhofer Institute for Solar Energy Systems located in Freiburg, Germany. The purpose of this comparison is to confirm whether the building model we adopted behaves similarly to an actual passively cooled building.

Fig. 6 illustrates a scatter plot of the average room air temperatures for the model and the measured data in the ISE building. It can be concluded that the indoor-to-outdoor air temperature relationship for both buildings is similar indicating that the energy balance of both the model and the actual building is similar, i.e., the change in heat stored as driven by sensible thermal gains and losses is correctly modeled. Moreover, the chart shows two enlarged triangular markers at ambient temperatures of approximately 30 °C: The lower marker reflects a room temperature of 26.7 °C at the beginning of the heat wave (hour 5125), while the upper marker reflects a room temperature of 30.1 °C towards the crest of the heat wave (hour 5206). Fig. 7 compares the time history of the average room air temperatures for the model and the measured data in the ISE building during the first week of the heat wave. The two sets of enlarged markers correspond to the same events in Fig. 6.

It is worth noting that the monthly average zone temperature is slightly lower for the case of the manipulated weather data, i.e., 27.86 °C versus 28.21 °C. Because of the consistent alternation of warm and cooler days in the case of the manipulated weather data, the building thermal storage inventory sees higher nighttime ventilation temperature differences that promote better discharging of the building thermal capacitance. Thus, in the case of the manipulated weather data, the building exhibits a smaller effective building thermal mass as the temperature disturbances do not penetrate the massive building structure as deeply as for the case of the original weather data with heat wave. From a system theoretic viewpoint, the heat wave represents a low-frequency excitation for which the building responds with a larger gain compared to the higher-frequency diurnal excitations. At the end of the simulation period, a steady-period condition has not been reached again. More time is necessary for the thermal

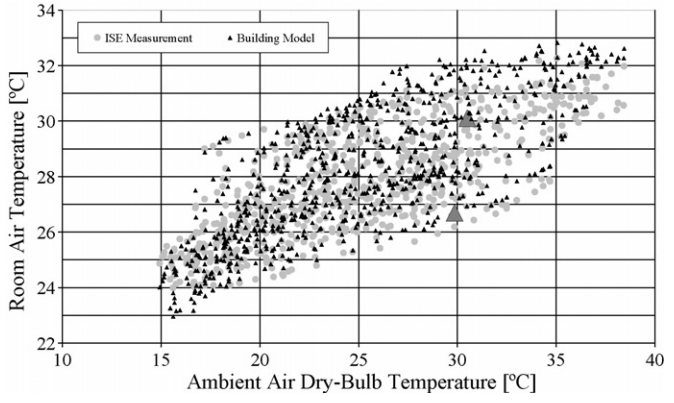

Fig. 6. Comparison of the passive building response for the building model and the Fraunhofer ISE using fixed ventilation schedules as a scatter plot. The average room temperature of the three south exposed building model zones is 28.21 °C compared with the average room temperature of the 15 measured south exposed offices in the Fraunhofer ISE building of 27.83 °C.

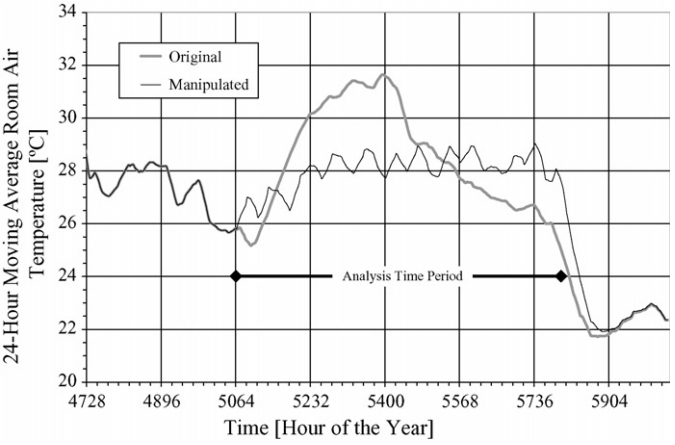

Fig. 8. Comparison of the 24-h moving average of the average building room air temperature for the original and manipulated weather data including a time period of identical weather preceding and following the analysis time period.

Table 3
Comparison of comfort violation frequency in the unconditioned building for the two adaptive comfort criteria for the case of original weather data with heat wave and the manipulated weather data without heat wave

Comfort criterion	Weather data			
	With heat wave		Without heat wave	
	Events	Frequency (%)	Events	Frequency (%)
prEN 15251	2420	21.7	2222	19.9
NPR-CR 1752	2648	23.7	2183	19.6

history of the heat wave to no longer impact the building response. As an illustration, Fig. 8 shows the 24-h moving average of the average room air temperature for a period before and after the analysis time period. It is evident that another 10 days of identical weather data are necessary for the room air temperature responses to converge again.

The impact of the heat wave can be quantified by evaluating the number of times (frequency) that a comfort criterion is violated. Based on 15 zones and 744 h in a 31-day period, there are 11,160 temperature-zone events. Table 3 illustrates the difference in comfort violation frequency assuming either of the adaptive comfort criteria (prEN 15251 and NPR-CR 1752) for the original weather data with heat wave and the manipulated weather data without heat wave. Once the building has been fully charged as a result of the heat wave, it takes longer to cool down again relative to the same building that experiences relatively cooler days after hot ones.

The effect of the building structure overheating during the heat wave is more closely examined for the case of the adaptive comfort criterion NPR-CR 1752 by comparing the simulated passive thermal building response of the three south-facing zones for the original weather data with heat wave against the manipulated weather data without heat wave. Fig. 9 depicts the room temperature versus the weighted moving average ambient temperature used in NPR-CR 1752 for the two weather data sets. It can be seen that the presence of the heat wave leads to higher reference temperatures and causes the building to reside for many hours at high room temperatures. Relative to the case without heat wave, there are more hours during which the comfort criterion is violated at those high values of the reference temperature because the building thermal storage inventory is depleted.

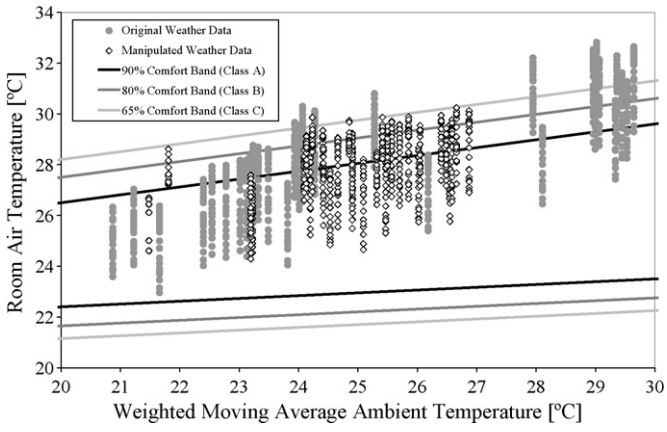

Fig. 9. Comparison of the simulated room air temperature vs. the weighted moving average ambient temperature used in NPR-CR 1752 for the two weather data sets for the passive thermal building response.

7. Optimal control modeling

7.1. Optimal control modeling

We adopt the following three optimization variables:

(1) A *precool period* Δt [h], counting from the beginning of occupied and on-peak time. For example, if the building is occupied as of 8:00, on-peak period begins at 11:00 and precooling begins at 5:00, then $\Delta t = 6$ h. The precool period can be chosen in 0.5 h time steps.
(2) During the precool period, depending on the relative onset of occupancy and on-peak utility rate periods, at most two of the following three *precool temperatures* can be selected
- Off-peak, unoccupied precool temperature setpoint $T_{\text{off,unocc}}$.
- Off-peak, occupied precool temperature setpoint $T_{\text{off,occ}}$.
- On-peak, unoccupied precool temperature setpoint $T_{\text{on,unocc}}$.

Occupancy is assumed to commence at 8:00, while the on-peak period begins at 11:00. Therefore, precool temperature setpoint $T_{\text{on,unocc}}$ is not available. The precool period Δt was varied in the range $0 \leq \Delta t \leq 14$ h. Counting backward in time, for the first 3 h of precooling (8:00–11:00), the lower and upper limit are 20 and 24 °C, while for precool periods $3 < \Delta t \leq 14$ h, the lower and upper limit are 15 and 35 °C.

Although peak demand charges can be accounted for in the objective function, this study only takes TOU energy charges into consideration. In fact, high on-peak energy charges can be envisioned to contain an incrementalized demand charge.

While it would be desirable to optimize the entire simulation horizon of 1 month, the nonlinearity of the optimization task

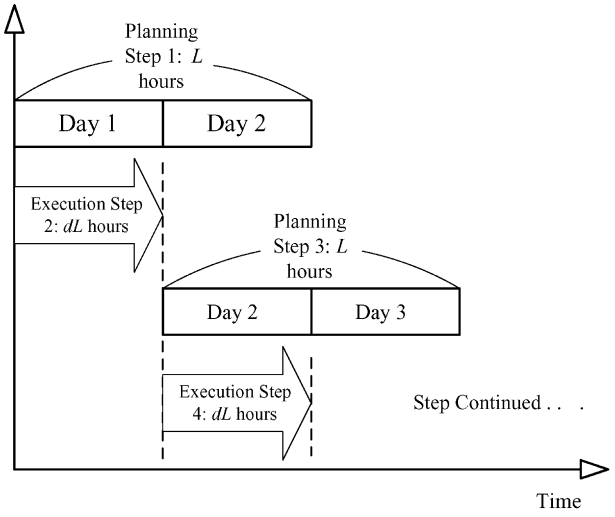

Fig. 10. Two-stage process for closed-loop predictive optimal control: planning and execution alternate.

and the high dimensionality associated with finding on the order of 100 optimal decision variables, invariably leads to the optimizer being caught in local minima. Thus, an alternative had to be found to more reliably find an optimal solution. The solution adopted in the context of this research was to employ closed-loop predictive optimal control.

The strategy of the optimization routine is to first define a planning horizon and an execution period, termed L and dL, respectively, and then carry out a two-stage process as shown in Fig. 10. During the planning stage, the optimizer first projects L hours into the future and calculates the optimal control setpoint for the entire planning horizon. Once an optimal solution has been found, the first $dL \leq L$ hours of the planned strategy are executed, i.e., the building simulation is carried out with the optimal setpoints and the thermal history at the end of the execution period becomes the initial thermal history at the beginning of the next planning stage. Optimization begins at the end of occupancy (18:00), so that the evening and morning hours are used for precooling before the on-set of the next expensive on-peak and occupied period.

The length of the planning horizon is an important decision variable. The larger the horizon over which the optimization is performed, the higher the dimensionality of the task and significantly longer optimization times are required; this leads to an excessive number of function evaluations. This in turn may cause the controller to get stuck in local minima and/or produce non-optimal control setpoints. On the other hand, the control decisions made for a particular day influence later decisions because the thermal time constant of the building is very long. Therefore, the correct choice of the planning horizon L is a trade-off between required optimization time, the likelihood of local minima, and the desire to optimize over horizons that are longer than the thermal time constant of the building. During the investigation it was found that $24 < L \leq 72$ leads to a good compromise. In the end, $L = 48$ h was selected.

During the dL-hour execution stage, the optimal control setpoint are merely evaluated in the simulation environment. It should be noted that dL must always be less than the planning horizon L as the execution period cannot be longer than the period for which an optimal solution was found. If $dL = L$, the controller believes that time ends after the selected planning window and therefore non-optimal control decisions will be made during the last hours of the defined window. One way of addressing this problem is to begin the planning horizon at the end of the occupied period so that the last few hours of the planning horizon are occupied hours. The purpose of building precooling is to shift daytime cooling loads to nighttime hours, so in effect, setting the end of the planning horizon to coincide with the end of occupancy ensures that the optimizer always sees the cooling loads to be shifted. Interestingly, in spite of this precaution, still marginally superior results were found when the optimizer sees two days ($L = 48$ h) instead of just 1 day ($L = 24$ h). The validity of the optimal solution was verified by means of a comparison with an exhaustive search for a steady-periodic case of 21 identical days [15].

7.2. Optimization algorithms and convergence criteria

Two minimization algorithms were tested and it was found that the Nelder-Mead Simplex method [28] ascertained the optimal solution more robustly for large numbers of cases compared to the quasi-Newton method developed by Broyden, Fletcher, Goldfarb, and Shanno [29]. Both methods found sensible solutions close to the benchmark optimum, but the Nelder-Mead Simplex method delivered consistently superior savings in spite of considerably longer run times. The results in the article were generated using the Nelder-Mead Simplex method. Due to the longer solution times required, the quasi-Newton method may be adopted in more time-critical applications such as real-time predictive optimal control.

Convergence criteria are additional parameters of choice when dealing with optimization tasks, and it was found that the convergence criteria must be considered in parallel with the planning horizon L due to the thermal history of the building. The best absolute convergence criterion was determined to be: $\varepsilon = 0.1$ for both the optimization variable (temperature) and the cost function (operating cost), i.e., the convergence is achieved when each temperature setpoint and the objective function vary by less than 0.05 K (0.1 times the increment of 0.5 K) or 0.1 US$/Euro, respectively.

8. Discussion of results

8.1. Results for conventional building control

Before describing the findings for the selected month of August, energy intensities for the entire cooling season (April through September 2003) are provided for the building model in order to better characterize the cooling-related building energy performance. Table 4 lists the cooling season energy intensities for the chiller (E_{CHLR}), the fans (E_{FANS}), lighting and equipment (E_{GAINS}), and the total electrical energy intensity (E_{TOTAL}) [kWh/m^{2}a] for comfort criterion ISO 7730 based on the gross floor area of 5184 m^2.

Next, we turn to the analysis of the results obtained for conventional nighttime setup control as the reference case. For the investigated time period of 1 month, Table 5 lists the monthly energy consumption for the chiller (P_{CHLR}), the fans (P_{FANS}), lighting and equipment (P_{GAINS}), and the total monthly electrical energy consumption (P_{TOTAL}) [kWh] for each of the three comfort criteria. In addition, the total cooling load (Q_{LOAD}) [kWh] and peak cooling load (Q_{MAX}) [kW] is provided as well.

Table 4
Cooling season energy intensities for the investigated building model for the time period April through September 2003 in Freiburg, Germany assuming nighttime setback control and comfort criterion ISO 7730

Intensity	Value [kWh/m^{2}a]
E_{CHLR}	18.61
E_{FANS}	1.44
E_{GAINS}	41.36
E_{TOTAL}	61.40

Table 5
Comparison of monthly electrical energy consumption [kWh] for chiller, fans, lighting and equipment, and the entire building as well as total cooling load [kWh] and peak cooling load [kW] for three comfort criteria under conventional nighttime setback control

Comfort criterion	P_{CHLR}	P_{FANS}	P_{GAINS}	P_{TOTAL}	Q_{LOAD}	Q_{MAX}
Original weather data						
ISO 7730	25684	1954	36319	63957	70949	342
prEN 15251	22992	964	36319	60275	61109	314
Δ ISO	−10%	−51%	0%	−6%	−14%	−8%
NPR-CR 1752	22763	1078	36319	60160	60648	324
Δ ISO	−11%	−45%	0%	−6%	−15%	−5%
Manipulated weather data						
ISO 7730	25379	1880	36319	63578	69888	328
Δ Ori	−1%	−4%	0%	−1%	−1%	−4%
prEN 15251	22635	921	36319	59875	59879	265
Δ ISO	−10%	−51%	0%	−6%	−14%	−19%
Δ Ori	−2%	−4%	0%	−1%	−2%	−16%
NPR-CR 1752	21950	1009	36319	59279	57853	290
Δ ISO	−14%	−46%	0%	−7%	−17%	−12%
Δ Ori	−4%	−6%	0%	−1%	−5%	−10%

From the table it can be seen that lighting dominates the whole-building electricity consumption, followed by the chiller power consumption, and as a distant third, the fan power consumption. Next, employing either adaptive comfort criterion (prEN 15251 or NPR-CR 1752) reduces the chiller power consumption by about 10% and the fan power consumption on the order of 45–51%. Across all cases, using adaptive comfort criteria leads to cooling load reductions of 14–17% and whole-building energy consumptions 6–7% below those values attained for the non-adaptive ISO 7730 (as indicated by Δ ISO).

The comparison of the weather data sets (as indicated by Δ Ori) reveals that breaking up the heat wave reduces the cooling load by 1–5%, which leads to chiller power reductions between 1 and 4% and fan power reductions between 4 and 6% depending on the comfort criterion.

Table 5 also reveals that the peak cooling load is reduced by 5–8% when adopting adaptive comfort criteria relative to the non-adaptive ISO 7730 (as indicated by Δ ISO) in the presence of heat waves; much larger reductions of 12–19% in peak cooling load can be observed for the case when the heat wave is broken up. For the same comfort criterion, the additional reduction for the manipulated versus original weather data (as indicated by Δ Ori) ranges from 4 to 16%. In other words, the presence of heat waves more strongly affects the peak cooling load rather than the total monthly cooling load under the premise of identical average monthly values for temperature, humidity, and insolation.

The development of cooling loads in connection to the development of the cooling setpoint temperature (shown in Fig. 5) can be clearly seen from Fig. 11, which compares the cooling load profiles for the three comfort criteria for the first week of the analysis (hour 5057 to 5225, i.e., July 30 to August 5, 2003) under nighttime setup control. As the ambient temperature rises sharply during the heat wave, so does the cooling setpoint for the adaptive standard NPR-CR 1752 and the resultant cooling load is reduced. During those times that

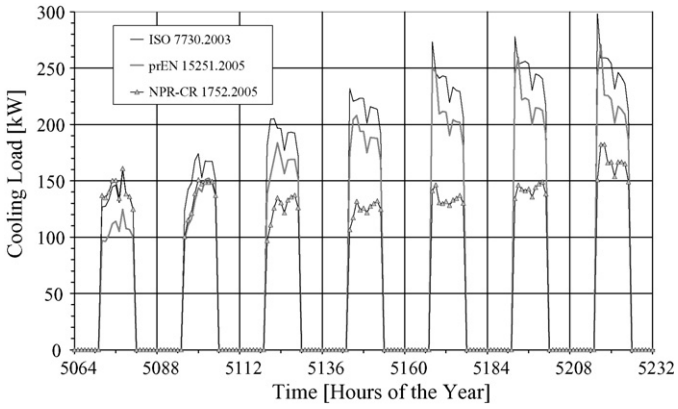

Fig. 11. Cooling load profiles for the three comfort criteria for the first week of the analysis (hour 5064 to 5232, i.e., July 30 to August 5, 2003) under conventional nighttime setup control.

the ambient temperature falls below the monthly average, the cooling loads will be above those for prEN 15251.

The equations for the cooling setpoint for the two adaptive comfort criteria are identical except for the definition of the ambient temperature they reference. prEN 15251 uses the average monthly temperature and NPR-CR 1752 a weighted average of the current and past three days. Since the monthly average of this weighted 4-day average approaches the monthly average ambient temperature, the monthly cooling load for both criteria is expected to be similar. Indeed, as Table 5 shows, monthly total cooling loads are similar for prEN 15251 and NPR-CR 1752. It is interesting to note that the impact of the weather pattern stability on the cooling loads and building systems energy consumption is marginal. There are no significant differences to be observed for the case of the original weather data including the heat wave and the manipulated weather data with the heat wave broken apart.

Table 6 summarizes the economic impact of employing non-adaptive versus adaptive comfort criteria. Most of the conclusions drawn for the energy comparison hold for the

Table 6
Comparison of monthly electricity costs for chiller, fans, lighting, and the entire building for three comfort criteria under conventional nighttime setback control [US$ or Euro]

Comfort criterion	K_{CHLR}	K_{FANS}	K_{LIGHTS}	K_{TOTAL}
Original weather data				
ISO 7730	4142	296	5480	9918
prEN 15251	3727	148	5480	9355
Δ ISO	−10%	−50%	0%	−6%
NPR-CR 1752	3701	163	5480	9343
Δ ISO	−11%	−45%	0%	−6%
Manipulated weather data				
ISO 7730	4104	286	5480	9870
Δ Ori	−1%	−3%	0%	0%
prEN 15251	3682	142	5480	9305
Δ ISO	−10%	−50%	0%	−6%
Δ Ori	−1%	−4%	0%	−1%
NPR-CR 1752	3587	152	5480	9220
Δ ISO	−13%	−47%	0%	−7%
Δ Ori	−3%	−6%	0%	−1%

cost comparison as well, i.e., there is no discernable impact of the weather pattern stability: Lighting and chiller costs dominate the total operating costs and savings of 6% of total operating costs can be attained by adopting adaptive comfort criteria. A comparison of the weather data sets (as indicated by Δ Ori) reveals that breaking up the heat wave leads to insignificant changes in total building operating cost between 0 and 1%, which is due to chiller cost reductions between 1 and 3% and fan cost reductions between 3 and 6% depending on the comfort criterion. The individual savings for chiller and fan costs track the reductions in energy use closely. This would not be the case if a greater amount of energy was consumed during unoccupied and off-peak hours.

In light of the peak cooling load reductions for adaptive comfort criteria as evidenced by Table 5, it is fair to assume that the benefit of adaptive comfort criteria goes beyond operating cost savings to include the possibility of capital cost savings as a result of chiller and other equipment downsizing.

8.2. Results for optimal building thermal mass control

To validate that the optimal controller identifies sensible strategies, we compared two solutions found for two different levels of internal gains, 10 and 20 W/m^2. Fig. 12 reveals that longer and more pronounced precooling is selected when internal gains are high as evidenced by the average zone air temperature profile for the 15 building zones. The occupied period cooling temperature setpoint is 26 °C followed by setup control until the onset of precooling (7 h before on-peak period for the case of high internal gains and 3 h in the case of low gains.) With higher cooling loads from internal gains, stronger load shifting is to be expected to take advantage of the utility rate incentives. While this is not strictly a validation, it does satisfy the plausibility check.

In this section we will first present the findings for optimal building thermal mass control in tabular form similar to the discussion for conventional control. Subsequently, we will discuss features of the optimal precool strategies. It should be noted that unlike the previous section that emphasized the impact of adaptive comfort criteria relative to the non-adaptive ISO 7730, the comparisons in this sections highlight the changes of optimal control relative to conventional nighttime setup (Δ NS) control for the same comfort criterion.

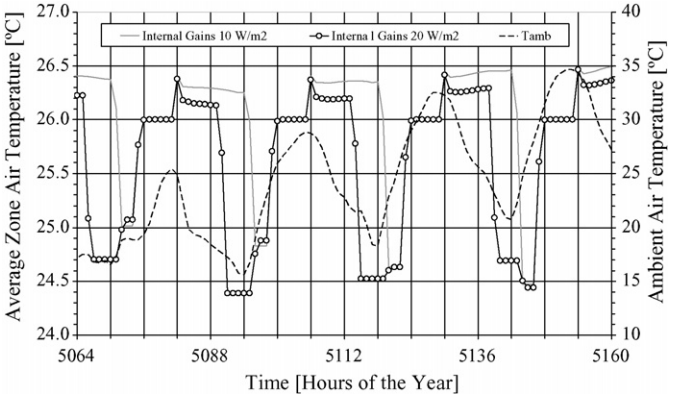

Fig. 12. Average zone air temperature [°C] profiles for two levels of internal gains under optimal building thermal mass control.

Table 7
Comparison of monthly electrical energy consumption [kWh] for chiller, fans, lighting and equipment, and the entire building as well as total cooling load [kWh] and peak cooling load [kW] for three comfort criteria under optimal building thermal mass control

Comfort criterion	P_{CHLR}	P_{FANS}	P_{GAINS}	P_{TOTAL}	Q_{LOAD}	Q_{MAX}
Original weather data						
ISO 7730	26481	2269	36319	65069	69437	454
Δ NS	3%	16%	0%	2%	−2%	33%
prEN 15251	23190	1279	36319	60789	58653	387
Δ NS	1%	33%	0%	1%	−4%	23%
NPR-CR 1752	22552	2734	36319	61605	61183	531
Δ NS	−1%	154%	0%	2%	1%	64%
Manipulated weather data						
ISO 7730	26029	2231	36319	64578	67949	388
Δ NS	3%	19%	0%	2%	−3%	18%
Δ Ori	−2%	−2%	0%	−1%	−2%	−15%
prEN 15251	22756	1229	36319	60304	57128	327
Δ NS	1%	33%	0%	1%	−5%	24%
Δ Ori	−2%	−4%	0%	−1%	−3%	−15%
NPR-CR 1752	21596	3037	36319	60953	58599	550
Δ NS	−2%	201%	0%	3%	1%	90%
Δ Ori	−4%	11%	0%	−1%	−4%	4%

From Table 7 it can be deduced that the cost-minimizing strategy leads to total building energy penalties between 1 and 3%, which is caused only by changes in chiller and fan energy use as the lighting and equipment schedules remain constant. In particular, chiller energy consumption varies between −2 and 3%, while fan power consumption increases sharply by 16 to 201%. Obviously, the additional fan use during nighttime precooling is responsible for most of the energy penalty.

The comparison of the weather data sets (as indicated by Δ Ori) reveals that breaking up the heat wave reduces the cooling load by 2–4%, which leads to chiller power reductions between

Table 8
Comparison of monthly electricity costs for chiller, fans, lighting, and the entire building for three comfort criteria under optimal building thermal mass control [US$ or Euro]

Comfort criterion	K_{CHLR}	K_{FANS}	K_{LIGHTS}	K_{TOTAL}
Original weather data				
ISO 7730	2990	135	5480	8606
Δ NS	−28%	−54%	0%	−13%
prEN 15251	2847	81	5480	8408
Δ NS	−28%	−45%	0%	−10%
NPR-CR 1752	3015	169	5480	8664
Δ NS	−19%	4%	0%	−7%
Manipulated weather data				
ISO 7730	2968	133	5480	8581
Δ NS	−28%	−53%	0%	−13%
Δ Ori	−1%	−1%	0%	0%
prEN 15251	2831	79	5480	8390
Δ ISO	−23%	−44%	0%	−10%
Δ Ori	−1%	−3%	0%	0%
NPR-CR 1752	2984	189	5480	8652
Δ ISO	−17%	24%	0%	−6%
Δ Ori	−1%	11%	0%	0%

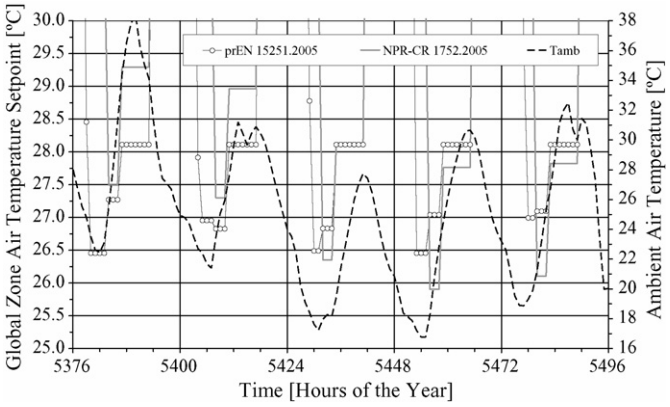

Fig. 13. Comparison of global zone temperature setpoint [°C] for the adaptive comfort criteria for the time period of hour 5376 to 5496.

2 and 4% and fan power changes between −2 and 11% depending on the comfort criterion.

It is apparent from Table 7 that optimal building thermal mass control leads to higher peak cooling loads and may thus require larger primary and secondary HVAC equipment.

Table 8 clearly demonstrates the potential economic benefits of building thermal mass control under optimal control. The monthly whole-building electricity cost savings for the non-adaptive comfort criterion ISO 7730 are 13% lower relative to conventional control for both weather data sets. As can be expected from the reduced cooling loads, savings from optimal control are less than for the non-adaptive comfort criterion: 10% for prEN 15251 and 6–7% for NPR-CR 1752. This result is surprising since the cost reductions resulting from either adaptive comfort criterion were nearly identical (6–7%) for conventional control (see Table 6).

Further analysis of these results revealed that the optimizer chooses distinctly different precooling strategies for the two adaptive comfort criteria that explain the differences in savings. Referring to Fig. 5, it can be seen that the weighted moving average reference temperature falls below the monthly average ambient temperature at around hour 5465 (as evidenced by lower cooling temperature setpoints). In the case of prEN 15251 the optimizer decides to adopt longer precool periods with higher precool temperature setpoints, while for NPR-CR 1752, the optimizer decides to use shorter precool periods with lower precool temperature setpoints as shown in Fig. 13. This decision results in sharp cooling load spikes and higher monthly peak cooling loads (Table 7). The peak cooling load for NPR-CR 1752 of Q_{MAX} = 531 kW occurs at hour 5480. These peak cooling loads occur during nighttime periods when demand rates normally do not apply.

While the impact of the adaptive comfort criterion of choice on the monthly total cost savings is significant, we can again observe no significant effect of weather pattern stability (as indicated by Δ Ori).

9. Summary and conclusions

This article evaluated the potential of building thermal mass control of commercial buildings to reduce utility costs with a particular emphasis on the impacts of adaptive comfort criteria and of heat waves. Recent changes in pertinent international standards on thermal comfort for indoor environments allow for some adaptation to the weather development. Changes in allowable temperature limits for the indoor environment will thus affect the energy consumed to operate the building energy systems under both conventional (nighttime setup) and optimal precooling operating strategies. Since extreme weather patterns tend to occur more frequently even in moderate climate zones, it was of concern how a building's passive thermal storage inventory responds to prolonged heat waves. The individual and compounded effects of adaptive comfort criteria and heat waves on the conventional and optimal operation of a prototypical office building were investigated for the particularly hot month of August 2003 in Freiburg, a city located in southwest Germany.

To arrive at meaningful findings, the methodology adopted in this work entails: selection of (a) a representative low-energy office building model and (b) weather data that contain sufficiently extreme features both in terms of average temperature as well the occurrence of multi-day heat waves; (c) calibration of the building model with measured data from an actual building to investigate whether the building adopted for this study is suitable for the application of adaptive comfort criteria; (d) selection of one standard (ISO 7730) and two adaptive comfort criteria (prEN 15251 and NPR-CR 1752); (e) conducting monthly simulations runs for both conventional nighttime setup control and optimal building thermal mass control for the selected two weather data sets and three comfort criteria. The results were evaluated by means of a monthly energy cost analysis utilizing a dynamic building energy simulation program coupled to a popular technical computing environment. Quantitative comparisons were presented for the conventional strategy and the cost-optimal building thermal mass precooling strategy.

The following findings for the impact of comfort criteria and heat waves on *conventional building operation* were generated:

(1) With and without heat waves, using adaptive comfort criteria leads to significant total cooling load reductions of 14–17% and whole-building energy consumptions 6–7% below those values attained for the non-adaptive ISO 7730, which is due to chiller power reductions of about 10% and fan power reductions of 45–51%.
(2) By comparison, the presence of heat waves has a relatively small effect on total cooling loads. Breaking up the heat wave reduces the total cooling load by 1–5%, which leads to chiller power reductions between 1 and 4% and fan power reductions between 4 and 6% depending on the comfort criterion.
(3) The peak cooling load is reduced by 5–8% when adopting adaptive comfort criteria relative to the non-adaptive ISO 7730 in the presence of heat waves; much larger reductions of 12–19% in peak cooling load can be observed for the case when the heat wave is broken up. Thus, the presence of heat waves more strongly affects the peak cooling load than the total monthly cooling load under the premise of identical

average monthly values for temperature, humidity, and insolation.

(4) Also in terms of cost, there is no discernable impact of the weather pattern stability under conventional control: lighting and chiller costs dominate the total operating costs and savings of 6% of total operating costs can be attained by adopting adaptive comfort criteria. Breaking up the heat wave leads to only insignificant changes in total building operating cost. The individual savings for chiller and fan costs track the reductions in energy use closely.

In contrast, when employing *optimal building thermal mass control* to harness the passive building thermal storage inventory, the following insights can be formulated:

(1) The cost-minimizing strategy leads to total building energy penalties between 1 and 3%, caused by changes in chiller and fan energy use. Here, the additional fan use during nighttime precooling is responsible for most of the energy penalty.
(2) As in the case of conventional nighttime setup control, the presence of heat waves has a relatively small effect on total cooling loads. Breaking up the heat wave reduces the total cooling load by 2–4%, which leads to chiller power reductions between 2 and 4% and fan power changes between −2 and 11% depending on the comfort criterion.
(3) Optimal building thermal mass control leads to higher peak cooling loads and may thus require larger primary and secondary HVAC equipment.
(4) The potential economic benefits of building thermal mass control under optimal control are significant: the monthly whole-building electricity cost savings for the non-adaptive comfort criterion ISO 7730 are 13% lower relative to conventional control for both weather data sets. As can be expected from the reduced cooling loads, savings from optimal control are less than for the non-adaptive comfort criterion: 10% for prEN 15251 and 6–7% for NPR-CR 1752.
(5) While the impact of the adaptive comfort criterion of choice on the monthly total cost savings is significant, again no significant effect of weather pattern stability can be observed.

Summarizing, adaptive comfort criteria strongly reduce total cooling loads and associated building systems energy consumption under conventional and building thermal mass control. In the case of conventional control, total operating cost reductions follow the cooling loads reductions. Conversely, the use of adaptive comfort criteria under optimal building thermal mass control leads for prEN 15251 to lower absolute operating costs and in the case of NPR-CR 1752 to slightly higher total costs compared to the optimal costs for ISO 7730. While the presence of heat waves strongly affects the peak cooling loads under both conventional and optimal building thermal mass control, total cooling loads, building energy consumption and costs are only weakly affected for both control modes. Passive cooling under cost-optimal control, while achieving significant total cost reductions of up to 13%, is associated with total energy penalties on the order of 1–3% relative to conventional nighttime setup control.

In conclusion, building thermal mass control defends its cost saving potential under optimal control in the presence of adaptive comfort criteria and heat waves. Even under conventional setup control will adaptive comfort criteria offer attractive energy and cost savings relative to non-adaptive standards. These savings, however, fall short of what is attainable using optimal building thermal mass control.

References

[1] J.E. Braun, Reducing energy costs and peak electrical demand through optimal control of building thermal mass, ASHRAE Transactions 96 (2) (1990) 876–888.
[2] A.A. Golneshan, M.A. Yaghoubi, Simulation of ventilation strategies of a residential building in hot arid regions of Iran, Energy and Buildings 14 (1990) 201–205.
[3] M.E. Snyder, T.A. Newell, Cooling cost minimization using building thermal mass for thermal storage, ASHRAE Transactions 96 (2) (1990) 830–838.
[4] A. Rabl, L.K. Norford, Peak load reduction by preconditioning buildings at night, International Journal of Energy Research 15 (1991) 781–798.
[5] I. Andresen, M.J. Brandemuehl, Heat storage in building thermal mass: a parametric study, ASHRAE Transactions 98 (1) (1992).
[6] K.R. Keeney, J.E. Braun, A simplified method for determining optimal cooling control strategies for thermal storage in building mass, International Journal of HVAC&R Research 2 (1) (1996) 59–78.
[7] J.P. Conniff, Strategies for reducing peak air-conditioning loads by using heat storage in the building structure, ASHRAE Transactions 97 (1) (1991) 704–709.
[8] F.B. Morris, J.E. Braun, S.J. Treado, Experimental and simulated performance of optimal control of building thermal storage, ASHRAE Transactions 100 (1) (1994) 402–414.
[9] M.E. Ruud, J.W. Mitchell, S.A. Klein, Use of building thermal mass to offset cooling loads, ASHRAE Transactions 96 (2) (1990) 820–828.
[10] K.R. Keeney, J.E. Braun, Application of building precooling to reduce peak cooling requirements, ASHRAE Transactions 103 (1) (1997) 463–469.
[11] J.E. Braun, T.M. Lawrence, C.J. Klaassen, J.M. House, Demonstration of load shifting and peak load reduction with control of building thermal mass, in: Proceedings of the 2002 ACEEE Conference, 2002.
[12] J. Pfafferott, S. Herkel, M. Jäschke, Design of passive cooling by night ventilation: evaluation of a parametric model and building simulation with measurements, Energy and Buildings 35 (11) (2003) 1129–1143.
[13] J. Pfafferott. Enhancing the design and operation of passive cooling concepts. Ph.D. dissertation, Fraunhofer IRB Verlag, Stuttgart, Germany, ISBN 3-8167-6626-9, 2004.
[14] G.P. Henze, D. Kalz, S. Liu, C. Felsmann, Experimental Analysis of Model-Based Predictive Optimal Control for Active and Passive Building Thermal Storage Inventory, International Journal of HVAC&R Research 11 (2) (2005) 189–214.
[15] G.P. Henze, T.H. Le, A.R. Florita. Sensitivity analysis of optimal building thermal mass control, in: Proceedings of the 2005 International Solar Energy Conference in Orlando, Florida, American Society of Mechanical Engineers.
[16] G.P. Henze, R.H. Dodier, M. Krarti, Development of a Predictive Optimal Controller for Thermal Energy Storage Systems, International Journal of HVAC&R Research 3 (3) (1997) 233–264.
[17] G.P. Henze, M. Krarti, The impact of forecasting uncertainty on the performance of a predictive optimal controller for thermal energy storage systems, ASHRAE Transactions 105 (1) (1999) 553–561.
[18] S. Liu, G.P. Henze. Impact of modeling accuracy on predictive optimal control of active and passive building thermal storage inventory. ASHRAE Transactions, Technical Paper No. 4683, 110(1), 2004, 151–163.
[19] J.E. Braun, Load control using building thermal mass, Journal of Solar Energy Engineering 125 (3) (2003) 292–301.

[20] Carrier Corporation. 30GTN air-cooled reciprocating liquid chillers with comfortlink controls, available for download at http://www.xpedio.carrier.com/idc/groups/public/documents/techlit/30gtn-5pd.pdf, 2003.
[21] U.S. Department of Energy. DOE-2 Reference Manual, Part 1, Ver. 2.1. Lawrence Berkeley Laboratory, 1980.
[22] C. Schär, G. Jendritzky, Hot news from summer 2003, Nature 432 (2004) 559–560.
[23] P.A. Stott, D.A. Stone, M.R. Allen, Human contribution to the European heatwave of 2003, Nature 432 (2004) 610–614.
[24] MeteoNorm v4.0. Global meteorological database for solar energy and applied climatology. MeteoTest, Bern, Switzerland, 1999.
[25] prEN ISO 7730:2005. Ergonomics of the thermal environment. Beuth Verlag, Berlin, 2005.
[26] prEN 15251:2005. Criteria for the indoor environment. Beuth Verlag, Berlin, 2005.
[27] A.C. van der Linden, A.C. Boersta, A.K. Raue, S.R. Kuvers, R.J. de Dear, Adaptive temperature limits: a new guideline in the Netherlands – a new approach for the assessment of building performance with respect to thermal indoor climate, Energy and Buildings 38 (1) (2006) 8–17.
[28] J.A. Nelder, R. Mead, A simplex method for function minimization, Computer Journal 7 (1965) 308–313.
[29] Matlab. Optimization Toolbox User's Guide. The MathWorks, Inc., 2006.